

Efficient Wideband Jammer Nulling When Using Stretch Processing

JOSE A. TORRES

RICHARD M. DAVIS, Senior Member, IEEE

J. DAVID R. KRAMER, Life Member, IEEE

RONALD L. FANTE, Fellow, IEEE
The MITRE Corporation

Techniques are described for performing adaptive jammer nulling over extremely wide bandwidths on radar systems which use linear frequency modulated (LFM) waveforms and stretch processing. It is assumed that the range uncertainty of the target is a small percentage of the equivalent range extent of the uncompressed pulse. The assumption allows the cancellation to take place following stretch processing in either the time domain using a narrowband sliding filter that keeps up with the chirp rate or in the frequency domain. The new approach supports nulling performance over gigahertz of bandwidth comparable to that previously achieved over a few megahertz using approximately the same number of spatial degrees of freedom.

Manuscript received May 13, 1999; revised March 16, 2000; released for publication May 1, 2000.

IEEE Log No. T-AES/36/4/11364.

Refereeing of this contribution was handled by J. P. Y. Lee and K. A. Normand.

Authors' address: The MITRE Corporation, 202 Burlington Rd., Bedford, MA 01730-1420.

0018-9251/00/\$10.00 © 2000 IEEE

I. BACKGROUND

Sidelobe cancellers are used to null interference received through the sidelobes of an antenna pattern [1]. The canceller obtains samples of the jamming signals from spatially separated auxiliary antennas. The samples are multiplied by complex weights and then summed and combined with the output of the main antenna to minimize the interference. Many algorithms exist for calculating the weights. It takes only one auxiliary antenna and one adaptive weight to null a single narrowband sidelobe jammer. We define a jammer to be narrowband if the antenna gain in the direction of the jammer can be represented as a constant independent of frequency. As the bandwidth of the jammer increases, its spectrum spreads through the sidelobes of the pattern so that each frequency is received with a slightly different gain. The number of sidelobes, which the jammer spreads through, is equal to the product of the difference in arrival time of the jammer plane wave across the face of the antenna with the jammer bandwidth. The product is referred to as the time-bandwidth (TB) product. The TB product of large microwave radars having ten or twenty percent tunable bandwidth can exceed ten.

A rule of thumb for traditional spatial cancellers is that it takes two adaptive weights (two auxiliary antennas) to cancel a jammer that spreads through a single sidelobe. Thus, it takes roughly $2TB_j$ adaptive weights to null J jammers using the traditional architecture. Since each adaptive channel requires a separate receiver and all of the receivers must be matched in amplitude and phase over the entire cancellation bandwidth, the traditional wideband adaptive processor quickly becomes cumbersome and costly. The limitations of three traditional approaches used to null over extremely wide bandwidths are described below.

Fig. 1 shows a hybrid implementation of a traditional spatial canceller in which the adaptive weights are calculated digitally and then applied

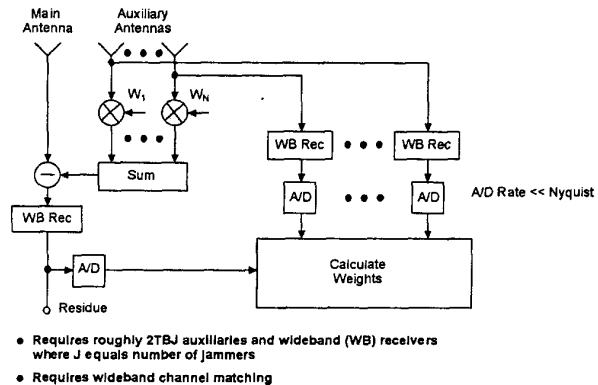


Fig. 1. Traditional approach 1: Spatial-only using hybrid architecture.

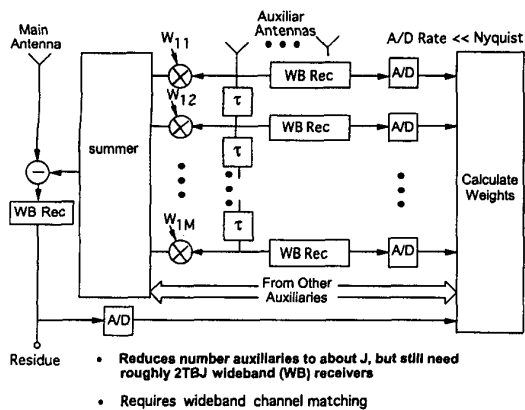


Fig. 2. Traditional approach 2: Space-time using hybrid architecture.

to analog modulators. Since the samples are only used to calculate the weights, which are determined by cross correlations, the analog-to-digital (A/D) sampling rate can be much less than Nyquist. The number of auxiliary antennas, or equivalently the number of independent spatial samples can be reduced by using the adaptive finite impulse response (FIR) filter implementation depicted in Fig. 2. The adaptive FIR filter, which is one form of space-time processing, is also a traditional approach [2]. The weights are chosen to make the shape of the filter mimic the frequency response of the jammer received through the sidelobes in the main antenna. The number of auxiliary antennas needs only be about equal to the number of jammers (J). The space-time filter, however, still requires roughly $2TBJ$ wideband receivers and adaptive weights. As with the spatial-only approach, the receivers must be matched in amplitude and phase over the cancellation bandwidth. The adaptive FIR filter can compensate for ripples in the frequency domain transfer function that are longer than $(M\tau)^{-1}$ Hz, where M is the number of taps. Ripples that are shorter than $(M\tau)^{-1}$ Hz, and do not track channel to channel, cannot be cancelled and will fundamentally limit performance.

It is noteworthy that if only a single wideband receiver were used in each auxiliary channel in Fig. 2 and followed by an A/D converter clocking at the Nyquist rate, the delays (τ) could be derived from the sampled data. The cancellation node and all subsequent processing, including pulse compression, would then have to be implemented digitally. Although converters that clock at a few gigahertz and have sufficient dynamic range may be available in the near term, the throughput requirement needed to multiply the adaptive weights by the auxiliary channel voltages in every range cell, and perform digital pulse compression in large numbers of beams per second, quickly becomes excessive.

A third traditional approach for attempting to null over extremely wide bandwidths is to divide

the bandwidth into subbands (SB_m) and operate an independent canceller in each one (see Fig. 3). The subbanding architecture reduces the number of required auxiliary antennas to roughly $2J$ and eliminates the requirement for wideband channel matching. However, the total required number of adaptive weights remains at about $2TBJ$.

II. POST-STRETCH PROCESSING CANCELLER

In this section, we show that wideband nulling becomes much easier on systems which use stretch processing. Stretch processing is a technique that enables the use of wideband waveforms with narrowband processing [3-4]. Stretch processing works best when the range uncertainty is a small fraction of the range extent of the uncompressed pulse. It entails transmitting a linear frequency modulated (LFM) waveform. The receive signal is mixed with a deramping oscillator having the same LFM slope as the transmitted waveform. If the deramper is started at the beginning of the range window, then target returns are translated into tones by taking the difference frequency out of the mixer. The frequency of the tones denotes the ranges to the targets. The combination of the deramper followed by a narrowband filter acts like a spectrum analyzer, converting range (time) into frequency. The target tones can be detected by taking a fast Fourier transform (FFT) after narrowband filtering and digitization. The minimum bandwidth of the narrowband filter following the deramper is given by the LFM slope times the maximum possible delay of a target return within the range window, i.e.,

$$B_{\text{MIN}} = \left(\frac{B}{T_u} \right) \frac{2\Delta R}{c} \quad (1)$$

where

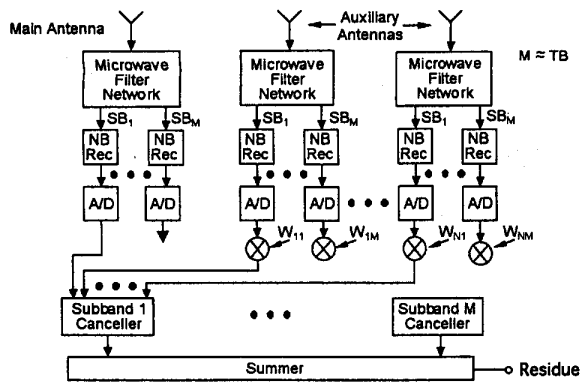
B = signal (chirp) bandwidth

T_u = uncompressed pulse width

ΔR = range uncertainty = range window

c = speed of light.

Let us assume that a sidelobe jammer is present which spreads its energy uniformly over the chirped bandwidth. If we insert a narrowband filter having bandwidth B_{MIN} in the receiver following the deramper, then at any instant of time, the output of the filter will display a slice of the jammer spectrum having width equal to B_{MIN} . Since B_{MIN} is typically much smaller than B , the entire jammer spectrum will slide through the filter window as time runs from zero to T_u seconds. The post-stretch processing canceller architecture supports efficient jammer nulling over extremely wide bandwidths in either the



- Reduces number auxiliaries to about 2J and eliminates wideband channel matching
- Requires microwave filter network, roughly 2TBJ narrowband (NB) receivers, and M cancellers

Fig. 3. Traditional approach 3: Subbanding.

time or frequency domains. In either case, there will be a significant reduction in the hardware needed to implement the canceller compared with traditional methods.

A. Equivalency to Traditional Subbanding and Space-Time Cancellers

Implementing sidelobe cancellation on a stretch processing system in the time domain is equivalent to the traditional subbanding approach depicted in Fig. 3. The left insert in Fig. 4 shows a computer simulation of the magnitude squared value of samples following the deramper and narrowband filter, but before the FFT in a stretch receiver. The jammer and LFM bandwidths (B) were each 1000 MHz, the narrowband filter bandwidth (B_{MIN}) was 20 MHz, and the uncompressed pulsewidth (T_u) was 100 μ s. The plot represents the response of a 264 element linear array to a Gaussian jammer having a TB product of 11.5. Although we are in the time domain, the samples out of the A/D converter show the jammer spectrum spreading through 11.5 sidelobes. The mapping from time to frequency brought about by the deramper and narrowband filter is shown at the top of the insert. The array was divided into subarrays with phase steering used within a subarray and time steering between them. The single high sidelobe is due to misalignment between the array factor and the subarray pattern as the subarray scans with frequency. The samples can be divided into blocks, where each block represents a subband, and a separate canceller can be implemented within each block. The main difference between the traditional subbanding approach shown in Fig. 3 and the left insert is that the subbands come for free and their width is controllable with stretch processing.

Taking the FFT of the picture in the left insert of Fig. 4 puts us in the frequency domain. However,

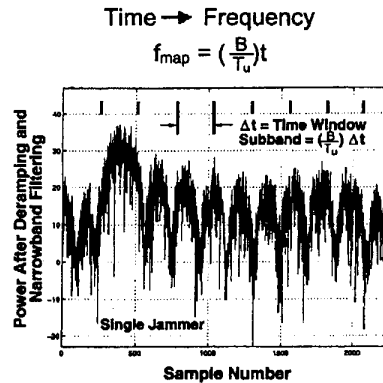
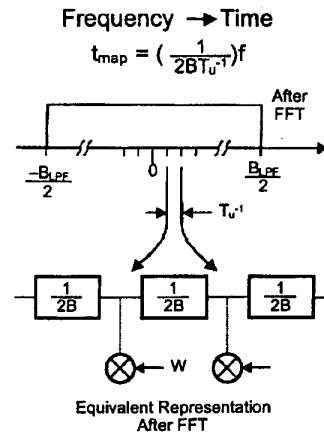


Fig. 4. Time-frequency mapping forces equivalency to traditional subband and space-time processing.

because of the mapping between frequency and time, the frequency bins correspond to range (time) cells, which can be represented as a tapped delay line with tap spacing $(2B)^{-1}$. Adaptively weighting a subset of the frequency bins in the auxiliaries to null a bin in the main channel is equivalent to the traditional space-time processing architecture shown in Fig. 2. It is noteworthy that the delays in the tapped delay line can be controlled (made smaller than B^{-1}) by zero padding the time domain samples before taking the FFT.

B. Post-Stretch Processing Canceller in Time Domain

There are two approaches for implementing the canceller in the time domain: 1) the sliding window approach, and 2) the multiple fixed window approach. Cancellation in the time domain takes place after the deramper and narrowband filter, but before the FFT (see Fig. 5). Although the cancellation bandwidth must be larger than B_{MIN} , we desire to keep it small enough so that we can null a single jammer using only two weights. As previously noted, the portion of the jammer spectrum that appears in the cancellation band is constantly changing as the deramping frequency slides across the signal

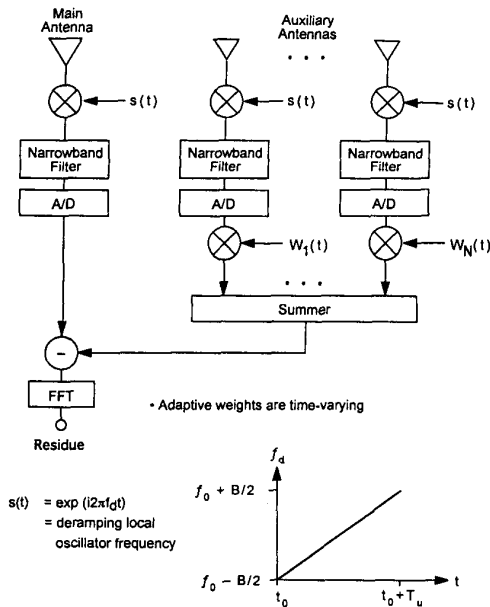


Fig. 5. Time domain post-stretch processing canceller.

bandwidth. Using the sliding window approach, the time-varying, adaptive weights must be changed fast enough to keep up with the changing filter response.

A recursive algorithm such as the least mean square (LMS) algorithm is well suited for determining the time-varying weights in the sliding window implementation [2]. The weights in the LMS algorithm are updated after each sample by adding a small increment to the old weights. The increment is proportional to the rate of change of the output residue power with respect to the weight being updated. The algorithm must be designed so that the weights change fast enough to keep up with the deramping local oscillator as it slides across the signal band at a rate of B/T_u Hz/s.

The canceller can also be implemented in the time domain by dividing all of the samples out of the A/D converters into multiple nonoverlapping fixed windows. The windows, as noted in the previous section, correspond to subbands. The samples in each window from the main and auxiliary channels are stored and either all or some of them are used to calculate the adaptive weights. The weights are applied retroactively to all of the auxiliary samples in the block. The weighted auxiliary samples are summed and subtracted from the samples in the main channel to null the interference. An algorithm such as sample matrix inversion (SMI) can be used to calculate the adaptive weights [5]. The SMI algorithm inverts the covariance matrix of the voltages in the auxiliary channels and multiplies it by the cross-correlation vector between the main and auxiliary channels to obtain the weights. Although windowing requires operating independent cancellers

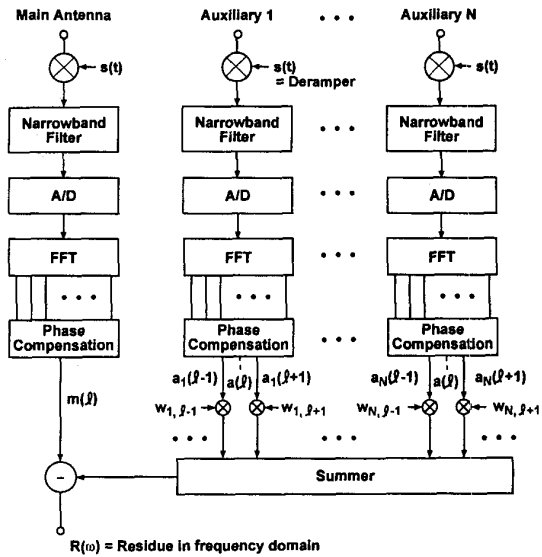


Fig. 6. Frequency domain post-stretch processing canceller.

on multiple data blocks, the receiver bandwidth and A/D conversion rates are low due to the post-stretch processing implementation. Since the blocks to be cancelled are separated in time, the data can be multiplexed through a single canceller.

C. Post-Stretch Processing Cancellor in Frequency Domain

The post-stretch processing canceller can also be implemented in the frequency domain. The frequency domain approach requires that the deramped data in the main and in each auxiliary channel, which has been narrowband filtered and digitized, be transformed into the frequency domain using an FFT. After transformation, the main and each auxiliary will typically consist of thousands of frequency bins, but only a small number of them correspond to the range window of interest. Since target returns will be above the thermal noise level after the FFT, we must either calculate the adaptive weights prior to transmission or use out-of-band correlation, to prevent the canceller from attempting to null target returns. The out-of-band correlation technique entails using a small number of frequency bins in the main channel and each auxiliary channel that are separated from the bins corresponding to the range window of interest to calculate the weights. Each main channel bin within the window of interest is cancelled by applying the weights to corresponding auxiliary channel bins located on either side of the main channel bin. The weighted bins are summed and subtracted from the main channel bin to be cancelled (see Fig. 6). Many algorithms, including the LMS and SMI, can be used to calculate the weights. The phase compensation process shown in Fig. 6 is discussed in the following analysis section.

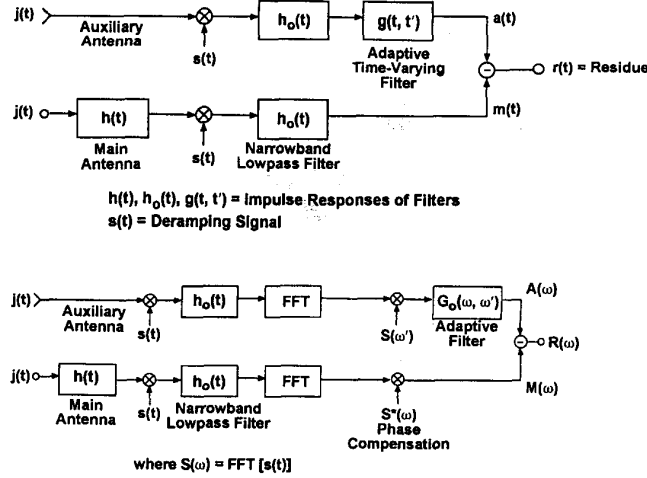


Fig. 7. Adaptive filters in time and frequency domains.

III. ANALYSIS

A. Adaptive Filters in Time and Frequency Domains

Fig. 7 shows block diagrams of the canceller being implemented in the time (top insert) and frequency (bottom insert) domains. The adaptive filter is modeled as a time-varying linear filter. The function $g(t, t')$ denotes the response of the time-varying filter at time t to an impulse occurring at time t' . If the system were not time varying, then the impulse response would only be a function of $t - t'$. The adaptive filter in the time domain could be found by setting $a(t)$ equal to $m(t)$ and solving for $g(t, t')$. An alternative approach is to first set the transfer function of the auxiliary channel $A(\omega)$ equal to the transfer function of the main channel $M(\omega)$ and solve for the frequency domain adaptive filter $G(\omega, \omega')$. In Fig. 7, we denote the frequency bin in the main channel, which is being cancelled by ω and the bin in the auxiliary channel, which is used to do the cancellation by ω' . The time domain filter $g(t, t')$ could be obtained by taking the inverse Fourier transform of $G(\omega, \omega')$. Assuming that the jamming signal is much larger than receiver thermal noise, the frequency domain adaptive filter can be shown to be equal to (see Appendix A for derivation)

$$G(\omega, \omega') = \gamma e^{-i(\gamma/2)(\omega^2 - \omega'^2)} G_0(\omega, \omega') \quad (2)$$

where

$$G_0(\omega, \omega') = h(\gamma(\omega' - \omega))$$

= adaptive filter without phase compensation,

$$\gamma = \frac{T_u}{2\pi B}$$

$h(t)$ = impulse response of main antenna

ω, ω' = radian frequency in main and auxiliary channels.

The phase compensation terms in (2) remove the quadratic phase terms due to the Fourier transform of the deramping signal $s(t)$ in the main and auxiliary channels. The adaptive filter is implemented by applying adaptive weights to frequency bins in the auxiliaries which are then summed and subtracted from one of the main channel bins. Since it is difficult for the weights to replicate the quadratic phase terms, we choose to remove them prior to adaptive processing. The phase compensation mixers shown in the bottom insert in Fig. 7 remove the phase terms (Fourier transform of deramping signals) in the main and auxiliary channels. Equation (2) can be factored to emphasize the fact that quadratic phase compensation can be performed prior to nulling:

$$G(\omega, \omega') = S(\omega') S^*(\omega) G_0(\omega, \omega') \quad (3)$$

where $S(\omega)$ is the Fourier transform of the deramping signal $s(t)$.

The functional form of (2) is particularly interesting. Substituting $G_0(\omega, \omega')$ into the filter box shown in Fig. 7 shows that a commutation relationship exists allowing the impulse response of the antenna to be placed at either the input or output to one of the channels. Given that ω is the center of the frequency bin in the main channel to be cancelled, (2) also tells us that the adaptive weights applied to frequency bins in the auxiliary channels are only a function of the frequency separation $\omega - \omega'$. In other words, once we derive the auxiliary channel weights to cancel one main channel frequency bin, we are able to cancel jamming in all other main channel bins by using those same weights (applied to different auxiliary frequency bins).

Equation (2) also tells us that the number of weights required to null the interference in a given bin in the main channel is determined by the effective length (the support) of the impulse response $h(\gamma\omega)$.

The support is typically small—about 5 to 10 frequency bins. Thus, the jamming can be removed from the range bins of interest by sliding a fixed set of 5 to 10 weights across the bins in each of the auxiliaries and then summing the outputs and subtracting from the main channel bin, while keeping the separation between the auxiliary and main channel bins fixed. The number of bins, which must be cancelled, depends upon the range window of interest.

There are a number of minimization techniques, which could be used to generate the adaptive weights needed to estimate $G_0(\omega, \omega')$. The authors used the SMI algorithm when generating the numerical results presented in Section IV. The weight vector in the SMI algorithm is well known to equal the inverse of the sample covariance matrix R of the auxiliaries times the cross-correlation vector P between the voltages in the main and auxiliary channels. The correlations needed to calculate the adaptive weights were performed out-of-band to prevent cancellation of desired target returns. The cross correlations which determine the R and P matrices used to calculate the adaptive weights depend only upon the difference in arrival time of the jamming between the two antennas being cross-correlated. The observation explains why only one set of auxiliary channel weights is needed to cancel the jamming in all main channel frequency bins. Examples of the cross correlations used in the R and P matrices are given in (4) and (5). Note that k can designate any one of the frequency domain taps as long as it is not one of the taps being cancelled (i.e., as long as it is out-of-band)

$$r((a_s(k), a_t(k + \ell)) = \frac{1}{M} \sum_{k=1}^M a_s(k) a_t^*(k + \ell) \quad (4)$$

$$p(m(k), a_t(k + \ell)) = \frac{1}{M} \sum_{k=1}^M m(k) a_t^*(k + \ell) \quad (5)$$

where

$a_s(k)$ = signal on k th frequency bin in s th auxiliary channel

$m(k)$ = signal on k th frequency bin in main channel

M = number of samples used to estimate the cross correlations.

The adaptive filter in the time domain can be obtained by taking the Fourier transform of (2). The analysis is outlined in Appendix B, where it is shown that

$$g(t, t') = 2\gamma \int_{-\pi B_0}^{\pi B_0} h(2\gamma x) e^{i(t+t')x} \times \frac{\sin[(2\gamma x - t + t')(\pi B_0 - |x|)]}{(2\gamma x - t + t')} dx \quad (6)$$

where

$$x = \frac{\omega' - \omega}{2}.$$

The sinc-like term in (6) represents the smoothing due to the finite bandwidth (B_0) in the narrowband filters $H_0(\omega)$. As B_0 becomes large, the narrowband filter is effectively removed from the system, the sinc-like term becomes an impulse $\delta(2\gamma x - t + \tau)$, and the adaptive filter reduces to

$$g(t, t') = \alpha h(t' - t) e^{i(t'^2 - t^2)/2\gamma} \quad (7)$$

where α is a scalar constant. Equation (7) is just what we would expect; it says that if the narrowband filter is removed, the adaptive weights in the auxiliary channels must match the impulse response of the main channel and remove the difference due to the deramping signals in the main and auxiliary channels.

B. Analysis of Signal Cancellation

Cancellation of target returns is not a problem in the frequency domain implementation because the correlations needed to calculate the adaptive weights are done out-of-band. Target cancellation, however, can be a problem in the time domain implementation. The target signal in the auxiliary channels can be ignored because the signal-to-noise ratio (SNR) in an auxiliary channel will be smaller than SNR in the main channel by the number of elements in the array. However, we cannot ignore the cross products between the jamming signal in the auxiliaries and target returns in the main channel. The cross-product terms will average to zero if we use enough samples when calculating the cross correlations. It is shown in Appendix C that the loss in signal power in the time domain implementation can be approximated as

$$L_s = 10 \log \left(1 - \frac{KN}{P} \right)^2 \quad (8)$$

where

N is the number of auxiliary channels

K is the number of nonoverlapping blocks of samples

P is the number of samples in FFT.

If, for example, we use 10 blocks and six adaptive elements and a 256-point FFT, the loss is predicted to be 2.3 dB. If the FFT is increased to 1024 points, the loss will only be 0.52 dB.

IV. NUMERICAL RESULTS

The post-stretch processing canceller was simulated in both the time and frequency domains. The SMI algorithm was used to calculate the adaptive weights. The radar waveform was modeled as a 100 μ s pulse chirped over 1000 MHz of bandwidth

at a center frequency of 7.0 GHz. After deramping, the bandwidth was reduced from 1000 to 20 MHz. The bandwidth reduction resulted in a processing gain of 17 dB (out of the full 50 dB) on the target return prior to A/D conversion. The remaining 33 dB of pulse compression gain occurred in the FFT following A/D conversion. A total of 2000 complex baseband digital samples were taken within the 100 μ s extent of the uncompressed pulse.

The simulation used a 264 element linear array divided into 12 subarrays of 22 elements each. Phase steering was used within a subarray and time steering between subarrays. The array was steered 30 deg off normal in all runs. The auxiliaries were chosen to be individual elements out of the array located at elements 1, 264, 97, 188, 102, 181, 241, and 260. The number of auxiliaries was varied from one to eight. No errors were included in the simulation. The number of jammers was varied from one to three. The complex baseband jamming waveforms were modeled as

$$j_{\ell m}(n) = P_j^{(1/2)} \left(\frac{x(n) + iy(n)}{\sqrt{2}} \right) \exp i[\omega(\tau_\ell - T_m) + \phi_\ell] \quad (9)$$

where

- n is the discrete time
- ℓ is the element within subarray
- m is the subarray
- P_j is the jammer power
- x, y are the zero mean, unit variance Gaussian variates
- τ_ℓ is the jammer arrival time relative to center of subarray
- T_m is the time delay steering applied to m th subarray
- ϕ_ℓ is the phase shift applied to ℓ th element in subarray
- ω is the radian frequency.

The jammers were located between 34 and 44 deg away from the steering direction, which resulted in BT products that varied from 10 to 13. The left insert in Fig. 4 showed a typical single jammer frequency response at the output of the A/D converter.

A. Numerical Results for Time Domain Canceller

Using the SMI algorithm, the samples out of the A/D converter were divided into nonoverlapping blocks (subbands) and a separate canceller was operated within each block. A number of sampling options were compared when forming the covariance matrix. Using all samples in a block provided the best performance. Using only $5N$ adjacent samples within a block (where N is the number of auxiliaries) to train the weights reduced the computational load,

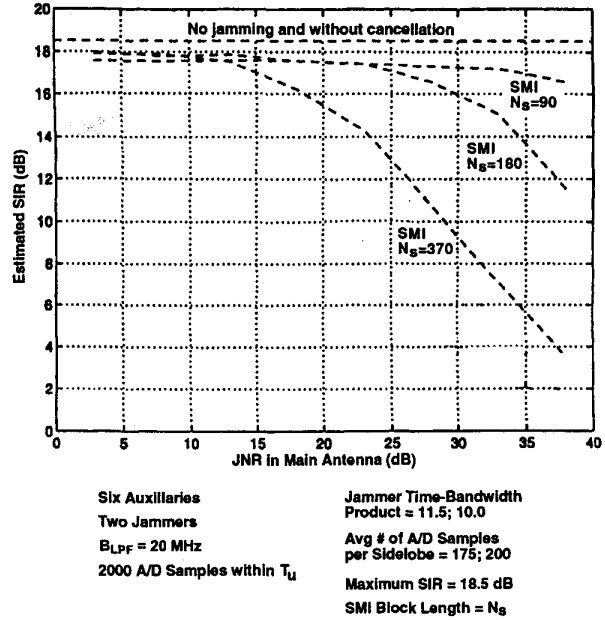
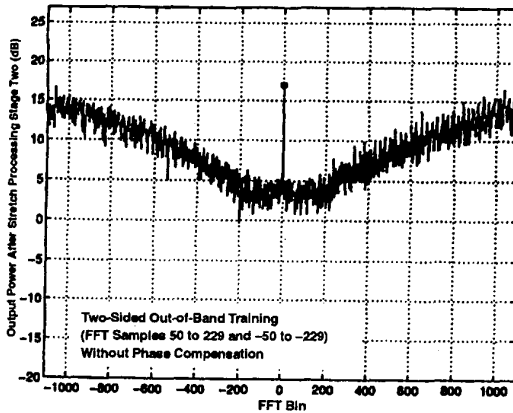
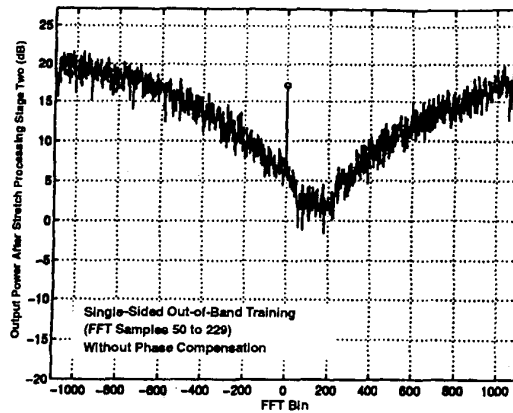


Fig. 8. Comparison of SMI algorithm using six auxiliaries and different block sizes operating against two jammers in time domain.

but also reduced performance. Using $5N$ nonadjacent samples distributed throughout a block reduced the computational load and maintained approximately the same level of performance as using all samples.

Fig. 8 compares the performance of block sizes consisting of 90, 180, and 370 samples. The blocks correspond to subbands spanning approximately one half, one, and two sidelobes, respectively. The canceller consisted of six auxiliaries and there were two jammers in the scenario. The number of samples per sidelobe was 175 for one of the jammers and 200 for the other. The figure plots signal-to-interference ratio (SIR) after pulse compression versus jammer-to-noise ratio (JNR) received in the main antenna. SIR is equivalent to dividing the target or SNR by the residue-to-noise-ratio after cancellation. SNR was 18.5 dB in the quiescent (no jamming) environment. All results represent the average of 50 Monte Carlo runs. The results show that for JNR ratios less than 25 dB, the block size can be chosen to be equal to the number of samples spanning approximately one sidelobe.

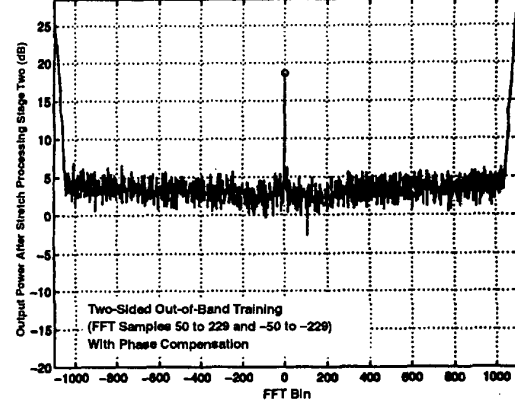
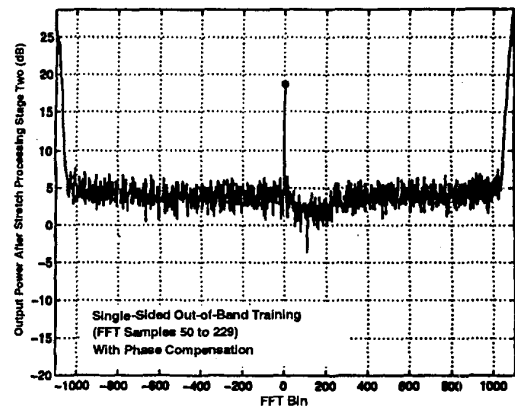
There was some concern that reassembly of the data blocks after removal of the jamming may impact the time sidelobe levels on the compressed pulse at the output of the final FFT. The impact of subbanding on the time sidelobes of the compressed pulse was found to depend upon the size of the subbands (blocks) and whether the system was overdetermined (more weights than needed to null the jammers). Small periodic anomalies were observed in the frequency domain at intervals of one over a subband. The problem became a little worse when the system



Three Auxiliaries
Single Jammer
 $B_{LPF} = 20$ MHz
2000 A/D Samples within T_{A}
Jammer Time-Bandwidth Product = 11.5

JNR in Main Antenna = 34 dB
Maximum SIR = 18.5 dB
Target Located at FFT Bin 0
Number of Adaptive Freq Bins = 12

Fig. 9. Three auxiliaries operating against one jammer in frequency domain without phase compensation.



Three Auxiliaries
Single Jammer
 $B_{LPF} = 20$ MHz
2000 A/D Samples within T_{A}
Jammer Time-Bandwidth Product = 11.5

JNR in Main Antenna = 34 dB
Maximum SIR = 18.5 dB
Target Located at FFT Bin 0
Number of Adaptive Freq Bins = 12

Fig. 10. Three auxiliaries operating against one jammer in frequency domain with phase compensation.

was heavily overdetermined. Diagonal loading the covariance matrix (see [6]) alleviated the problem in the overdetermined case. We conclude that, to first order, time domain processing with the sidelobe canceller architecture investigated in this study does not degrade compressed pulse time sidelobe levels.

B. Numerical Results for Frequency Domain Canceller

Figs. 9 and 10 show typical results when the canceller is implemented in the frequency domain. Results are presented for three auxiliaries operating against a single jammer where we have used the SMI algorithm to calculate the adaptive weights. The figures plot the output power in each of the 2000 frequency bins. A target return is shown in bin zero. Fig. 9 does not include the quadratic phase compensation while Fig. 10 does. Twelve frequency bins in each of the three auxiliaries surrounding the bin to be cancelled in the main channel were weighted, summed, and subtracted from the bin in

the main channel. The process was repeated in each of the 2000 bins using the same set of 36 weights. The range window of interest was between bins -50 and $+50$. The weights were trained on only one side of the range window in the top insert, but on both sides in the bottom insert. The residue within the range cells of interest was lower when we used two-sided out-of-band training. In the absence of phase compensation, the cancellation performance deteriorates as one moves away from the bins used to train the weights.

Fig. 11 shows performance of the frequency domain canceller operating against three jammers where the number of adaptive frequency bins was varied from seven to nine. Eight auxiliaries were used to null the jammers. The curves plot SIR versus JNR. The SIR values obtained using SMI in the time domain are also shown on the figure for comparison. The results represent an average of 50 Monte Carlo runs. The cancellation performance obtained in the time and frequency domains is comparable.

V. SUMMARY

We have demonstrated the feasibility of nulling sidelobe jammers over extremely wide bandwidths on systems which use stretch processing. The proposed technique exploits the mapping between time and frequency implicit in stretch systems. It was shown that nulling could be performed in the time or frequency domains. Nulling in the time domain takes place at the output of a narrowband filter. The jammer spectrum slides through the filter during the arrival time of the uncompressed pulse. The time domain approach is analogous to traditional cancellers which use subbanding, while the frequency domain approach is analogous to space-time processing.

It was shown that the transfer function of the auxiliary channels can be made identical to that of the main antenna by applying a filter to the spectrums of the auxiliary channels equal to the impulse response of the main antenna. The argument of the impulse response was shown to depend only upon the frequency difference between the main channel bin being cancelled and the auxiliary bin that is weighted and subtracted from the main channel bin. The observation showed that once a set of frequency domain weights is found that nulls a single frequency bin in the main channel, those same weights can be applied to other frequency bins in the auxiliaries to null any other bin in the main channel.

APPENDIX A. DERIVATION OF FREQUENCY DOMAIN ADAPTIVE FILTER

Referring to Fig. 7, $A(\omega)$ and $M(\omega)$ are given by

$$A(\omega) = \int d\omega' G(\omega', \omega) H_0(\omega') \int d\omega'' J(\omega'') S(\omega' - \omega'') \quad (10)$$

$$M(\omega) = H_0(\omega) \int d\omega'' J(\omega'') H(\omega'') S(\omega - \omega''). \quad (11)$$

Since we desire the residue $R(\omega)$ to be zero, we must have $A(\omega) = M(\omega)$ for arbitrary $J(\omega)$. Setting (10) equal to (11), we obtain

$$\int d\omega'' J(\omega'') \left[H_0(\omega) H(\omega'') S(\omega - \omega'') - \int d\omega' G(\omega', \omega) S(\omega' - \omega'') H_0(\omega') \right] = 0. \quad (12)$$

We next assume that we can represent the Fourier transform of the deramping signal $s(t) = e^{i(t^2/2\gamma)}$ by $S(\omega) \simeq e^{-i(\gamma/2)\omega^2}$ where $\gamma = T_u/2\pi B$. Equation (12) then

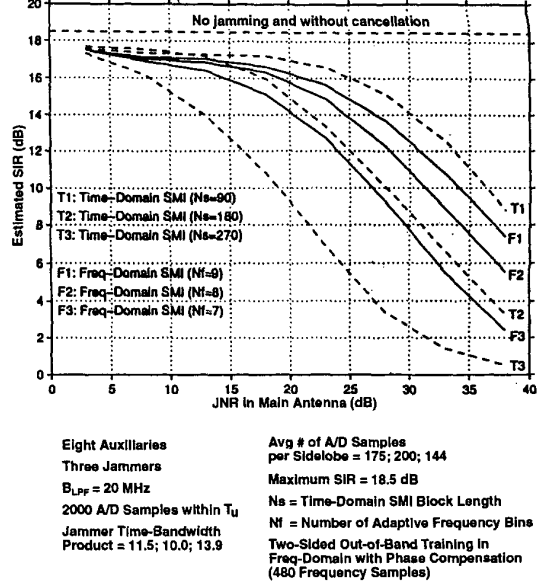


Fig. 11. Comparison of three jammer cancellation performance in time and frequency domains using SMI algorithm.

becomes

$$0 = \int d\omega'' J(\omega'') e^{-i(\gamma/2)\omega''^2} \times \left[H_0(\omega) H(\omega'') e^{-i(\gamma/2)(\omega^2 - 2\omega\omega'')} - \int d\omega' G(\omega', \omega) H_0(\omega') e^{-i(\gamma/2)(\omega'^2 - 2\omega'\omega'')} \right]. \quad (13)$$

Since $J(\omega'')$ is arbitrary, the term within the square bracket must be zero. Define $\tilde{G}(\omega', \omega) = e^{-i(\gamma/2)\omega^2} G(\omega', \omega)$ and multiply the square bracket in (13) by $(d\omega''/2\pi) e^{-i\gamma\Omega\omega''}$ and integrate. Noting that the integral over ω'' , in the term on the right is a Kronecker delta function, we obtain

$$H_0(\omega) e^{-i(\gamma/2)\omega^2} \frac{1}{2\pi} \int d\omega'' H(\omega'') e^{i\omega''\gamma(\omega - \Omega)} = \frac{1}{\gamma} \tilde{G}(\Omega, \omega) H_0(\Omega). \quad (14)$$

Since $h(t) = (1/2\pi) \int d\omega'' H(\omega'') e^{i\omega''t}$ and if $H_0(\omega) = 1$ for $-B/2 \leq \omega \leq B/2$, then

$$G(\Omega, \omega) = \gamma e^{-i(\gamma/2)(\omega^2 - \Omega^2)} h(\gamma(\omega - \Omega)) \quad (15)$$

where $-B/2 \leq \Omega \leq B/2$. In order to be consistent with the notation used in Fig. 7, we let $\Omega = \omega$ and $\omega = \omega'$ to obtain

$$G(\omega, \omega') = \gamma e^{-i(\gamma/2)(\omega^2 - \omega'^2)} h(\gamma(\omega' - \omega)). \quad (16)$$

Substituting $S(\omega)$ for the quadratic terms

$$G(\omega, \omega') = S(\omega')S^*(\omega)G_0(\omega, \omega') \quad (17)$$

where

$$G_0(\omega, \omega') = \gamma h(\gamma(\omega' - \omega)). \quad (18)$$

APPENDIX B. DERIVATION OF TIME DOMAIN ADAPTIVE FILTER

We derive the time domain filter by taking the inverse transform of the frequency domain filter

$$\begin{aligned} g(t, t') &= \int_{-\pi B_0}^{\pi B_0} \int_{-\pi B_0}^{\pi B_0} G(\omega, \omega') e^{i\omega t} e^{i\omega' t'} d\omega d\omega' \\ &= \gamma \iint h(\gamma(\omega' - \omega)) e^{i(\gamma/2)(\omega^2 - \omega'^2)} e^{i(\omega t + \omega' t')} d\omega d\omega' \end{aligned} \quad (19)$$

letting $x = (\omega + \omega')/2$, and $y = (-\omega + \omega')/2$, and adjusting the integration limits

$$\begin{aligned} g(t, t') &= 2\gamma \int_{-\pi B_0}^{\pi B_0} h(2\gamma x) \int_{-\pi B_0 + |x|}^{\pi B_0 - |x|} \\ &\quad \times e^{i2\gamma xy} e^{i(x-y)t} e^{i(x+y)t'} dy dx. \end{aligned}$$

Carrying out the integration over y ,

$$\begin{aligned} g(t, t') &= 2\gamma \int_{-\pi B_0}^{\pi B_0} h(2\gamma x) e^{i(t+t')x} \\ &\quad \times \frac{\sin[(2\gamma x - t + t')(\pi B_0 - |x|)]}{(2\gamma x - t + t')} dx. \end{aligned} \quad (20)$$

APPENDIX C. ANALYSIS OF SIGNAL CANCELLATION

The target return in the auxiliary channels can be ignored in the time domain implementation because SNR in an auxiliary channel will be smaller than SNR in the main channel by the number of elements in the array. However, we cannot ignore the cross products between the jamming signal in the auxiliaries and target returns in the main channel. The loss in signal power due to the cross terms is calculated below.

The analysis assumes that the canceller is implemented in the time domain. The samples out of the A/D converter are divided into K blocks (K subbands) and each block has its own canceller. The canceller is depicted in Fig. 12. The same canceller could be used for all blocks by multiplexing the data through it. The auxiliary vector space V can be transformed into the orthogonal vector space E by the similarity transformation A as depicted in Fig. 12. The row space of A are the eigenvectors of the covariance matrix of the input vector space V . The

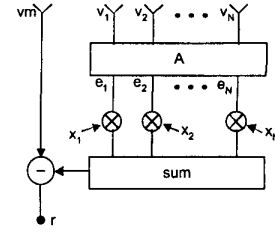


Fig. 12. Cancellor with orthogonalized auxiliary vector space.

eigenvectors form a basis for the input vector space and are, therefore, mutually uncorrelated.

The adaptive weights within each block are uncoupled. The weights for the k th block, for example, are

$$x_{kn} = \frac{\sum_{m=1}^M e_{kn}^*(q) v_m(q)}{\sum_{m=1}^M |e_{kn}(q)|^2}, \quad n = 1, N \quad (21)$$

where

$$q = (k-1)(P/K) + m = \text{time index}$$

M is the number samples used to estimate weights

P is the total number of time samples out of A/D converter spanning all blocks

K is the number of blocks = number of cancellers.

It should be noted that the number of samples (M) used to calculate the weights, in any given block, can be less than the total number of samples (P/K) in the block. In our analysis we have assumed that we always use the first M samples in a block to calculate the weights. The voltage in the main channel $v_m(q)$ is equal to the sum of the signal (target return) plus jamming plus thermal noise in the main channel. We assume that the jamming is completely cancelled and calculate the loss in signal power due to the cross terms between signal in the main channel and jamming in the auxiliary channels. We also assume that the signal in the auxiliaries is far enough below thermal noise so that it can be ignored. We also assume that the signal and jamming are large enough to allow us to ignore thermal noise in the analysis. Assuming that the jamming is completely cancelled, the residue which remains in the k th block is

$$r_k(q) = s(q) - \sum_{n=1}^N w_{kn} e_{kn}(q) \quad 1 < k \leq K \quad (22)$$

where

$$w_{kn} = \frac{\sum_{m=1}^M e_{kn}^*(q) s(q)}{\sum_{m=1}^M |e_{kn}(q)|^2} \quad (23)$$

and $s(q)$ is the signal (target return) in the main channel. We assume in our analysis that $s(q)$ is constant. Our objective is to calculate the loss in signal power after we perform the FFT (the last stage of stretch processing). The analysis to follow assumes we perform a discrete Fourier transform (DFT).

Taking a P -point DFT across the residue voltages $r_k(q)$, we obtain

$$G(p) = \sum_{k=1}^K \sum_{m=1}^{P/K} \left[s(q) - \sum_{n=1}^N w_{kn} e_{kn}(q) \right] e^{i(2\pi q(p-1)/P)}. \quad (24)$$

We can find the coherent part of $G(p)$ by taking its expectation

$$\begin{aligned} \langle G(p) \rangle &= \sum_{k=1}^K \sum_{m=1}^{P/K} \langle s(q) \rangle e^{i(2\pi q(p-1)/P)} \\ &\quad - \sum_{k=1}^K \sum_{m=1}^{P/K} \sum_{n=1}^N \langle w_{kn} e_{kn}(q) \rangle e^{i(2\pi q(p-1)/P)}. \end{aligned} \quad (25)$$

Using (23), and the approximation $\langle a/b \rangle \approx \langle a \rangle / \langle b \rangle$

$$\langle w_{kn} e_{kn}(q) \rangle = \frac{\sum_{m'=1}^M \langle e_{kn}^*(q') e_{kn}(q) \rangle \langle s(q') \rangle}{\sum_{m'=1}^M \langle |e_{kn}(q')|^2 \rangle} \quad (26)$$

where $q' = (k-1)(P/K) + m'$.

If the normal mode voltages $e_{kn}(q)$ are white noise random processes and we assume that the time samples are separated by at least an inverse bandwidth then

$$\langle e_{kn}^*(q') e_{kn}(q) \rangle = \langle |e_{kn}|^2 \rangle \delta_{q'q} \quad (27)$$

and

$$\begin{aligned} \langle w_{kn} e_{kn}(q) \rangle &= \frac{1}{M} s(q) \quad \text{for } (k-1)\frac{P}{K} < q \leq (k-1)\frac{P}{K} + M \\ &= 0 \quad \text{for } q \leq (k-1)\frac{P}{K} \quad \text{or} \\ &\quad q > (k-1)\frac{P}{K} + M. \end{aligned} \quad (28)$$

Substituting (28) into (25)

$$\begin{aligned} \langle G(p) \rangle &= \sum_{k=1}^K \sum_{m=1}^{P/K} \langle s(q) \rangle e^{i(2\pi q(p-1)/P)} \\ &\quad - \frac{1}{M} \sum_{k=1}^K \sum_{m=1}^M \sum_{n=1}^N \langle s(q) \rangle e^{i(2\pi q(p-1)/P)}. \end{aligned} \quad (29)$$

Assuming $s(q) = 1$ for all q , the target return will appear at zero frequency and show up in the first frequency bin $p = 1$ and

$$\langle G(1) \rangle = P - KN = \left(1 - \frac{KN}{P} \right) P. \quad (30)$$

The loss in target signal power is then

$$L = 10 \log \left(1 - \frac{KN}{P} \right)^2. \quad (31)$$

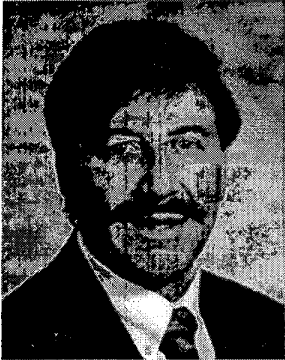
REFERENCES

- [1] Howells, P. W. (1965) Immediate frequency sidelobe cancellor. U.S. Patent 3202990, Aug. 24, 1965.
- [2] Widrow, B., Mantey, P. E., Griffiths, L. J., Goode, B. B. (1967) Adaptive antenna systems. *Proceedings of the IEEE*, **55**, 12 (Dec. 1967).
- [3] Caputi, W. J. (1971) Stretch: A time transformation technique. *IEEE Transactions on Aerospace and Electronic Systems*, **AES-7**, 2 (Mar. 1971).
- [4] Nathanson, F. E., Reilly, J. P., and Cohen, M. N. (1991) *Radar Design Principles* (2nd ed.). New York: McGraw Hill, 1991, 605-610.
- [5] Reed, I. S., Mallett, J. D., and Brennan, L. E. (1974) Rapid convergence rate in adaptive antennas. *IEEE Transactions on Aerospace and Electronic Systems*, **AES-10**, 6 (Nov. 1974).
- [6] Carlson, B. D. (1988) Covariance matrix estimation errors and diagonal loading in adaptive arrays. *IEEE Transactions on Aerospace and Electronic Systems*, **24**, 4 (July 1988).



Jose A. Torres received the B.S. degree in electrical engineering from Rensselaer Polytechnic Institute, Troy, NY, in 1984, and the M.S. degree in electrical engineering from Northeastern University, Boston, in 1989. He is currently a candidate for a Ph.D. degree in electrical engineering at Northeastern University.

He joined MITRE in 1986 where he is now a Principal Digital Signal Processing Engineer. He has developed adaptive digital signal processing algorithms and high performance computing architectures for radar and communications systems. From 1984 to 1986, Mr. Torres was employed by the Westinghouse Electric Corporation as a systems engineer, where he supported the development and modification of microprocessor-based subsystems that monitor the operational status of nuclear powered submarines.



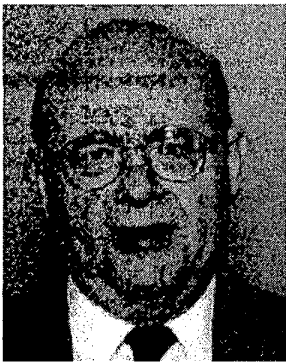
Richard M. Davis (S'62—M'71—SM'85) received the B.S.E.E. degree from the University of Rochester, Rochester, NY, in 1964, and the M.S.E.E. and B.A. degrees from Syracuse University, Syracuse, NY, in 1968 and 1975, respectively.

From 1964 to 1965, he was employed at the IBM Systems Development Division, Communications Laboratory, Raleigh, NC. Between 1966 and 1990, he worked for the Syracuse Research Corporation (SRC), Syracuse, NY. From 1984 to 1990, at SRC he was the Technical Director of the Analytical Studies Center which specializes in electronic counter countermeasures. He is currently a Senior Principal Engineer with the MITRE Corporation in Bedford, MA. His research interests are in the area of signal and adaptive processing.

J. David R. Kramer, Jr. received the bachelor's degree in electrical engineering from the University of Pennsylvania, Philadelphia, in 1957. He received the M.S.E.E. in 1958 and the Doctor of Science in 1964, both from the Massachusetts Institute of Technology, Cambridge.

He has been a consultant to the Rand Corporation and has served as instructor and lecturer at MIT and Northeastern University. In 1964 he joined the technical staff of The MITRE Corporation. He was named Consulting Scientist in 1983. During his career at MITRE, he has worked on a large variety of radar and communications systems. He has worked on ballistic missile defense, artillery locating radar, missile warning radar, and air defense radar. He was involved with JTIDS, HAVE QUICK, SEEK TALK, and other jam resistance communications systems. He has worked in electromagnetic propagation, signal processing, and target tracking. He has lead MITRE projects in the areas of adaptive antennas, HF experimentation, and target tracking. He developed methods of wideband signal processing and adaptive processing for the mitigation of HF atmospheric noise and clutter. He has also participated in studies of advanced ECM and ECCM techniques. Dr. Kramer's recent work has been in the evaluation of discrimination algorithms for the National Missile Defense system, and he has participated in various conceptual studies concerned with applying spacing based radar techniques to complement, supplement (or ultimately replace) conventional method of detecting, tracking and identifying airborne and ground targets.

Dr. Kramer, Jr., is a member of Tau Beta Pi and Eta Kappa Nu.



Ronald L. Fante (M'59—SM'72—F'79) holds a B.S. from the University of Pennsylvania, Philadelphia, an M.S. from Massachusetts Institute of Technology, Cambridge, and a Ph.D. from Princeton University, Princeton, NJ.

He is a Fellow of The MITRE Corporation and is active in electromagnetics and signal processing. Dr. Fante is a former editor of the IEEE Transactions on Antennas and Propagation.

Dr. Fante is also a Fellow of the Optical Society of America and the Institute of Physics.